

Fig. 2 Laminar heat-transfer rate ratio for a 15°-semi-angle blunt cone at three angles of attack

² Vaglio-Laurin, R., "Laminar heat transfer on blunt-nosed bodies in three-dimensional hypersonic flow," Wright Air Development Center TN 58-147 (1958).

³ Lees, L., "Laminar heat transfer over blunt-nosed bodies at hypersonic flight speeds," *Jet Propulsion* 26, 259-269, 274 (1956).

⁴ Aerodynamics Staff, "Experimental laminar heat transfer distribution on a blunted 15° circular cone at angle of attack," General Applied Sciences Laboratories, TR 153 (March 1960).

⁵ Aerodynamics Staff, "Laminar heat transfer to the most windward ray of a 15° spherically blunted cone at angle of attack," General Applied Sciences Laboratories, TR 157 (April 1960).

Insulation Requirements for Long-Time Low-Heat Rate Environments

D. M. TELLEP* AND T. D. SHEPPARD†

Lockheed Missiles and Space Company, Sunnyvale, Calif.

PORTIONS of lifting vehicles entering the earth's atmosphere at satellite and supersatellite speeds experience low heat rates for comparatively long durations. Heat rates of 10 to 50 Btu/ft²-sec for periods ranging up to 2000 sec are not uncommon on afterbodies and leeward surfaces. In this environment, a thermal protection system of the type shown in Fig. 1 often is considered in preliminary design analyses. It consists of a low-density, low-conductivity inorganic foam applied to a metallic load-carrying substrate.

If the foam does not undergo thermal decomposition or experience oxidation reactions, the performance of such a

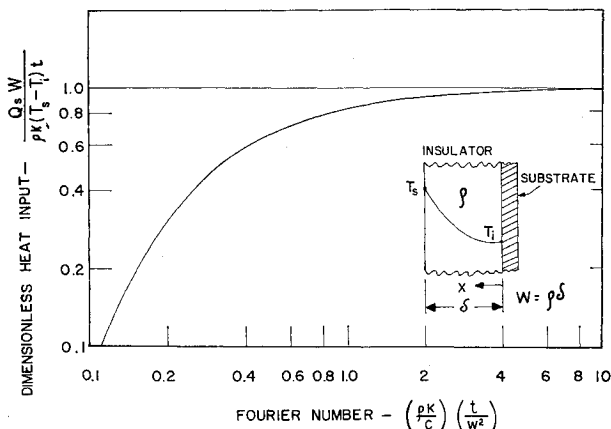


Fig. 1 Heat transmitted to rear surface of slab, the surfaces of which are maintained at constant temperatures

Received March 15, 1963.

* Manager, Launch and Entry Thermodynamics.

† Research Specialist.

system can be analyzed simply on the basis of a transient heat conduction analysis. This note presents an analysis that relates the weight per unit area of the insulation to the allowable temperature rise of the substrate in terms of the thermal properties of insulation and the heating environment.

The heating environment is characterized by a square heat pulse with a magnitude \dot{q} and a duration t . Stagnation enthalpy is considered to be much greater than the wall enthalpy. The heated surface of the low-density, low-conductivity insulator rapidly reaches a temperature near the radiation equilibrium value $(\dot{q}/\epsilon\sigma)^{1/4}$. As heat diffuses through the insulation into the substrate, the temperature of the inner surface of the insulation gradually rises. Normally, however, the allowable temperature rise of the substrate is small in comparison to the heated surface temperature. An upper bound for the heat transmitted to the substrate can be obtained by solving the diffusion equation for the insulation, subject to the boundary conditions

$$T(0,t) = T_i$$

$$T(\delta,t) = T_s \simeq (\dot{q}/\epsilon\sigma)^{1/4} \quad (1)$$

$$T(x,0) = T_i$$

Surprisingly, the solution to the transient heat conduction equation under the simple boundary conditions just given is not contained in standard heat conduction texts such as Carslaw and Jaeger. The solution was obtained by conventional methods to determine temperature-time histories in the insulation, subject to the assumption of constant thermal properties.

The quantity of primary interest is the integrated heat input to the substrate, Q_s . This is determined by differentiating the solution for $T(x,t)$ with respect to x , multiplying by the thermal conductivity, integrating with respect to time, and evaluating the result at the insulation-substrate interface. The result is

$$Q_s = \int_0^t k \left. \frac{\partial T}{\partial x} \right|_{x=0} d\tau = \frac{\rho k (T_s - T_i) t}{W} \times \left\{ 1 + \frac{2}{\pi^2 (\rho k/c) (t/W^2)} \sum_{n=1}^{\infty} \frac{(-1)^n}{n^2} \times \left[1 - \exp\left(- (n\pi)^2 \frac{\rho k}{c} \frac{t}{W^2}\right) \right] \right\} \quad (2)$$

where ρ , k , and c are the density, thermal conductivity, and specific heat of the insulation, respectively, and W is the section weight $\rho\delta$. The result expressed by Eq. (2) is shown in dimensionless form in Fig. 1. The Fourier number has been written in the form $(\rho k/c)(t/W^2)$ to emphasize the significant thermal property grouping when weight per unit area rather than thickness is used to characterize the insulation. In general, the pulse duration, surface temperature, and the allowable heat input to the substrate are considered known quantities, and the problem is to determine the insulation weight per unit area. This information can be obtained from the results shown on Fig. 1.

For Fourier numbers in excess of 3, the dimensionless heat input is close to unity, indicating that near-steady conduction prevails over the duration of the heat pulse. In this case, the required section weight is simply

$$W = \rho k (T_s - T_i) t / Q_s \quad (3)$$

The foregoing result also indicates that, for long-time, low-heat rate conditions, the required section weight for a given insulator depends more strongly on the pulse duration and allowable heat input to the substrate than on the integrated cold wall heat input $\dot{q}t$, since

$$W = \frac{\rho k [(\dot{q}t/\epsilon\sigma)^{1/4} - T_i t^{1/4}] t^{3/4}}{Q_s} \simeq \frac{\rho k (\dot{q}t)^{1/4} t^{3/4}}{(\epsilon\sigma)^{1/4} Q_s} \quad (4)$$

The results presented also emphasize the importance of low values of $\rho k/c$ in order to achieve minimum insulation weight.

Boundary Conditions at the Outer Edge of the Boundary Layer on Blunted Conical Bodies

VICTOR ZAKKAY* AND EGON KRAUSE†

Polytechnic Institute of Brooklyn, Freeport, N. Y.

IN most boundary layer analyses for blunted conical bodies the entropy gradient produced by the curved shock usually is neglected. However, Refs. 1 and 2 have pointed out that the boundary layer characteristics may be affected appreciably by this entropy variation, which influences the development of the boundary layer in two different ways. First, it causes a continuous change of the flow properties at the edge of the boundary layer in the streamwise direction, and second, it produces a velocity gradient at the outer edge in the normal direction, i.e., $(\partial u/\partial y)_e \neq 0$. In this investigation, only the streamwise variation at the edge of the boundary layer will be considered; thus, by assuming that $(\partial u/\partial y)_e \approx 0$, the local similarity concept can be applied.

The method developed herein is based on mass flow conservation inside the boundary layer and provides a convenient means of determining the variation of the flow properties at the outer edge of the boundary layer due to the local entropy gradient. Assuming local similarity, the mass flow equation as given by Lees³ can be applied for the laminar portion of the boundary layer. The external conditions at the edge of the boundary layer then can be determined by comparing the mass flow imbedded in the boundary layer with the mass flow in front of the shock entering at freestream conditions.

For a thermally and calorically perfect gas, the mass flow inside the boundary layer is

$$\dot{m} = 2^{3/2}\pi \left[(h_{01})^{1/2} \rho_{01} \mu_{01} R_0^3 \int_0^{\bar{s}} \bar{u}_e \bar{\mu}_e \bar{\rho}_e \bar{r}^2 d\bar{s} \right]^{1/2} f(\eta_e) \quad (1)$$

The mass flow in front of the shock at freestream conditions may be expressed as

$$\dot{m} = \rho_\infty u_\infty \pi \bar{y}^2 R_0^2 \equiv \dot{\omega} \quad (2)$$

If Eqs. (1) and (2) are used to eliminate $\dot{\omega}$, there results an equation for the normalized shock coordinate \bar{y} , corresponding to a station \bar{s} , namely,

$$\bar{y} = Z R_0^{-1/4} \left(\int_0^{\bar{s}} \bar{u}_e \bar{\mu}_e \bar{\rho}_e \bar{r}^2 d\bar{s} \right)^{1/2} \quad (3)$$

where

$$Z = \left\{ 2^{3/2} f(\eta_e) \frac{[(h_{01})^{1/2} \rho_{01} \mu_{01}]^{1/2}}{\rho_\infty u_\infty} \right\}^{1/2} \quad (4)$$

Equations (3) and (4) lead to a similarity parameter $\bar{s}'/Re_\infty^{1/4}$,

Received by IAS August 1962; revision received May 10, 1963. This research was sponsored by the Aeronautical Research Laboratories, Office of Aerospace Research, U. S. Air Force, under Contract AF 33(616)-7661, Project 7064 and is supported partially by the Ballistic Systems Division. A detailed discussion of these results is presented in Ref. 5.

* Research Associate Professor, Aerospace Institute. Member AIAA.

† Exchange Student, Aerospace Institute, from Institut fuer Angewandte Gasdynamik, DVL, Germany.

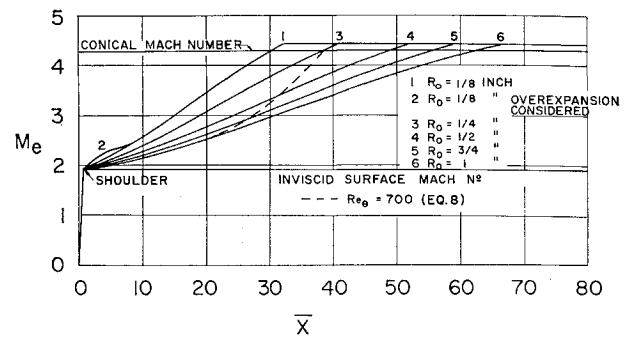


Fig. 1 Mach number distribution on blunt conical bodies; $M_\infty = 7.9$, $Re_\infty = 2.02 \times 10^6$ ft, $T_0 = 1660^\circ R$, $P_0 = 600$ psi, $\theta_b = 20^\circ$

as given in Ref. 2, where \bar{s}' is the normalized coordinate measured from the apex of the cone and Re_s is the local Reynolds number, based on the normal shock stagnation conditions; $Re_s = [\rho_{01}(h_{01})^{1/2}/\mu_{01}]\bar{s}'$. If this parameter is introduced, the dependence of the external flow properties on the nose radius vanishes.

When the shock shape in the form of an analytic expression $\bar{y} = f(\bar{x})$ and the distribution of the static pressure on the surface of the body are known, the local stagnation pressure at the edge of the boundary layer can be determined by solving the integral in Eq. (3) in a stepwise procedure. The local velocity \bar{u}_e , viscosity $\bar{\mu}_e$, and density $\bar{\rho}_e$, normalized with respect to the normal shock stagnation conditions, are given by the ratio of the local static-to-stagnation pressure. The static pressure in the nose region may be approximated by the modified Newtonian distribution, whereas on the conical portion of the body the static pressure is well represented by the pointed cone value. The observed overexpansion behind the shoulder on a blunted cone has only a little influence at high freestream Reynolds numbers but becomes more important when Re_∞ decreases.

Figure 1 presents the results of an application of this method; shown is the variation of the local Mach number external to the boundary layer on the conical portion of a spherically capped cone for various nose radii R_0 and for constant unit Reynolds number in the freestream, plotted vs the axial coordinate \bar{x} .

The results shown in Fig. 1 plus additional results given in Ref. 5 for a variety of flow conditions and nose radii indicate that the Mach number external to the boundary layer increases almost linearly until it finally approaches the value given by the surface Mach number of the pointed cone. With this approximation, Eq. (3) can be integrated to yield an approximate expression for the swallowing distance, i.e., the distance in which the external Mach number increases to the conical value, in terms of the flow parameters and the cone half angle. This expression may be found as follows. Simplifying the equation for the contour of the body $\bar{r} = \cos\theta_b + (\bar{s} - \bar{s}_c) \sin\theta_b$ to

$$\bar{r} = \bar{s} \sin\theta_b \quad (5)$$

and assuming a viscosity variation

$$\mu_e = \lambda T_e^{1/2} \quad (6)$$

where λ is introduced in order to match Sutherland's equation, one obtains for \bar{s}_c

$$\bar{s}_c \approx \left[\frac{3}{2} \frac{(R/\gamma)^{1/2}}{\lambda p_c} \frac{\rho_\infty^2 u_\infty^2}{(3M_e + M_s)} \frac{\bar{y}_c^4 R_0}{f^2(\eta_e) \sin\theta_b} \right]^{1/3} \quad (7)$$

where the integration is performed in the limits

$$\begin{aligned} \bar{s} &= 0 & M_e &= M_s \\ \bar{s} &= \bar{s}_c & M_e &= M_c \end{aligned}$$

A comparison between the foregoing approximation and the